

Luminosity Function of Morphologically Classified Galaxies in the Sloan Digital Sky Survey

Osamu Nakamura¹, Masataka Fukugita^{1,2}, Naoki Yasuda³, Jon Loveday⁴, Jon Brinkmann⁵, Donald P. Schneider⁶, Kazuhiro Shimasaku⁷, Mark SubbaRao⁸

ABSTRACT

The morphological dependence of the luminosity function is studied using a sample containing approximately 1500 bright galaxies classified into Hubble types by visual inspections for a homogeneous sample obtained from the Sloan Digital Sky Survey (SDSS) northern equatorial stripes. Early-type galaxies are shown to have a characteristic magnitude by 0.45 mag brighter than spiral galaxies in the r^* band, consistent with the ‘universal characteristic luminosity’ in the B band. The shape of the luminosity function differs rather little among different morphological types: we do not see any symptoms of the sharp decline in the faint end for the luminosity function for early-type galaxies at least 2 mag fainter than the characteristic magnitude, although the faint end behaviour shows a slight decline ($\alpha \lesssim -1$) compared with the total sample. We also show that a rather flat faint end slope for early-type galaxies is not due to an increasing mixture of the dwarf galaxies which have softer cores. This means that there are numerous faint early-type galaxies with highly concentrated cores.

Subject headings: cosmology: observations — galaxies: fundamental parameters

¹Institute for Cosmic Ray Research, University of Tokyo, Kashiwa 2778582, Japan

²Institute for Advanced Study, Princeton, NJ 08540, U. S. A.

³National Astronomical Observatory, Mitaka, Tokyo 1818588, Japan

⁴Astronomy Centre, University of Sussex, Brighton BN1 9QJ, United Kingdom

⁵Apache Point Observatory, Sunspot, NM 88349, U. S. A.

⁶Department of Astronomy and Astrophysics, Pennsylvania State University, University Park, PA 16802, U. S. A.

⁷Department of Astronomy, University of Tokyo, Tokyo 1130033, Japan

⁸Astronomy and Astrophysics Center, University of Chicago, Chicago, IL 60637, U. S. A.

1. Introduction

The origin of morphology of galaxies is a long-standing issue, which could provide a key to discerning among models of the formation of galaxies. How galaxy morphology changes as a function of the lookback time is perhaps the prime approach to this problem, and the knowledge of the morphological dependence of the local luminosity function at zero redshift is the baseline. One specific example of the issues is whether the luminosity function of elliptical galaxies obeys the Schechter-type function with a rather flat faint end (e.g., Marzke et al. 1994; Kochanek et al. 2001), or the Gaussian function as inferred by Binggeli, Sandage & Tammann (1988) and more recently by Bernardi et al. (2002a). If the latter is correct, one would envisage galaxy morphology as a bulge-luminosity sequence (Dressler & Sandage 1983; Meisels and Ostriker 1984), which in turn reveals a clue about the formation of elliptical galaxies and bulges.

There are also a number of uses of the morphology-dependent luminosity function (MDLF). We mention only one example: the frequency of gravitational lensing of quasar images is approximately proportional to the luminosity density of early-type galaxies rather than that of all galaxies (Fukugita & Turner 1991). The uncertainty in the MDLF is the largest source of error in predicting the frequency of gravitational lenses, and thus in inferring the cosmological constant from such analyses.

The understanding of the MDLF is significantly poorer than that of the luminosity function for galaxies in general, which has undergone substantial progress in the latest years (Folkes et al. 1999; Blanton et al. 2001) by virtue of large galaxy samples. The traditional way to obtain MDLF is to use morphological classification based on visual inspections of the images (Binggeli et al. 1988; Loveday et al. 1992; Marzke et al. 1994; 1998; Kochanek et al. 2001). Some modern studies attempt to use spectroscopic features to classify galaxies into morphological types (Bromley et al. 1998; Folkes et al. 1999), which makes it possible to analyze large samples. Although a general correlation is known between spectroscopic and Hubble morphologies, the samples derived from the two methods are considerably different. In particular, the classification using spectroscopic features or colours is sensitive to small star formation activities now or in the near past in early-type galaxies, whilst Hubble morphology is insensitive to this process. The problem of automated classification always lies in the difficulty in finding quantitative measures that strongly correlate with the Hubble sequence based on visual inspections. In this paper we derive the MDLF based on visual classifications using a homogeneous bright galaxy sample from Sloan Digital Sky Survey (SDSS; York et al. 2000). The sample we use in this paper is small, but it is based on a homogeneous morphological classification with accurate photometry.

The SDSS conducts both photometric (Gunn et al. 1998; Hogg et al. 2001; Pier et al.

2002) and spectroscopic surveys, and is producing a homogeneous data set, which is suitable to studies of galaxy statistics. The initial survey observations were made in the northern and southern equatorial stripes, and produced a galaxy catalogue to $r^* = 22.5$ mag in five colour bands (Fukugita et al. 1996) with a photometric calibration using a new standard star network observed at USNO (Smith et al. 2002). Spectroscopic follow-up is made to 17.8 mag with accurately defined criteria for target selection (Strauss et al. 2002).

Our study is limited to bright galaxies with $r^* \leq 15.9$ mag after Galactic extinction correction, since visual classifications sometimes cannot be made confidently beyond this magnitude with the SDSS imaging data. We have classified all galaxies satisfying this magnitude criterion in the northern equatorial stripe. The total number of galaxies in our sample is 1875, of which 1600 have spectroscopic information.

The dominant part of the data we used are already published as an *Early Data Release* (EDR) (Stoughton et al. 2002). Our present work uses primarily the EDR but supplemented by observations which are not included in EDR to make the sample as complete as possible. Photometry of galaxies in this region is discussed in a galaxy number count paper of Yasuda et al. (2001), and the luminosity function is derived by Blanton et al. (2001), which also discuss spectroscopic details.

2. The sample and the morphology classification

The region of the sky we consider is the northern equatorial stripe (SDSS photometry run numbers 752 and 756) for $145.15^\circ \leq \alpha(\text{J2000}) \leq 235.97^\circ$ and $|\delta(\text{J2000})| \leq 1.27^\circ$, which is included in the EDR sample. The total area is 229.7 square deg. We apply Galactic extinction correction using the extinction map of Schlegel, Finkbeiner & Davis (1998) assuming $R_{r^*} = A_{r^*}/E(B - V) = 2.75$, and select galaxies with the Petrosian magnitude $r^*_P \leq 15.9$ after the correction in the automatically-generated photometric catalogue (Stoughton et al. 2002). We use the extinction-corrected Petrosian magnitude throughout this paper.

The photometric catalogue yields 2418 galaxy candidates with $r^*_P \leq 15.9$ if we follow the criteria given in Strauss et al. (2002). This sample still contains number of double stars and shredded galaxies due to deblending failures, which cannot be rejected by the automated algorithm. We obtain after visual inspection of all galaxy candidates 1875 galaxies, of which 1600 (85%) are included in the spectroscopic sample. Spectroscopy was made using 50 plugged plates with additional 41 plates that are centred in the neighbouring stripes. These plates cover 228.1 square deg. The confidence level for the redshift determination is mostly over 99%, but 9 galaxies are given low ($< 85\%$) confidence, which we omit from our sample.

We also drop 38 galaxies which either contain multiple galaxies or have poor photometry due to deblending failures. This leaves 1553 galaxies. We note that there are some galaxies which are dropped in the primary galaxy selection in the photometric catalogue (Yasuda et al. 2001; Strauss et al. 2002) due to saturation flags caused by nearby bright stars or to other reasons. We estimate that we have probably missed about ≈ 88 galaxies in our field from the rate of missed galaxies given in Yasuda et al. So the overall sample completeness is estimated to be 79.5%. For more detailed discussion for the spectroscopic sample, see Blanton et al. (2001).

All galaxies in our sample (1875) are classified into 7 morphological classes, $T = 0$ (corresponding to E in the Hubble type), 1 (S0), 2 (Sa), 3 (Sb), 4 (Sc), 5 (Sd), and 6 (Im). Morphology classification is carried out by two of us (MF and ON) using the g^* band image of each galaxy displayed on the SAOimage viewer, according to *Hubble Atlas of Galaxies* (Sandage 1961). We also refer to morphological types given by the *Third Reference Catalogue of Bright Galaxies* (de Vaucouleurs et al. 1991; RC3), so that our classification closely matches to the traditional scheme, although the RC3 classification, which is based on the photographic material, is occasionally incorrect when galaxies are viewed with the CCD image, with which we can look at the image with different levels of brightness and contrast. We give an index of -1 when we cannot assign a morphological type. The classification by the two independent visual inspections agrees to within $\Delta T \leq 1.5$ for most galaxies and a mean (0.5 step in T) is taken for our final classification.

We reclassify galaxies into three groups of T , $0 \leq T \leq 1.0$ (E-S0), $1.5 \leq T \leq 3$ (S0/a-Sb), and $3.5 \leq T \leq 5$ (Sbc-Sd). The morphological distributions of the galaxies in the different samples are given in Table 1. The ratio of E-S0:S0/a-Sb:Sbc-Sd:Im $\simeq 0.40:0.34:0.24:0.02$. This is a somewhat larger fraction of E-S0 compared to the value usually adopted due to our use of r^* colour as the prime passband. For the same reason the fraction of Im galaxies is smaller by a factor of 2-3 than that from B selected samples. In this work we do not divide the morphology into further detailed classes considering the uncertainty in visual classification, especially between E and S0 for fainter galaxies. We consider $T > 5$ galaxies separately, since the spectroscopic target selection is biased against low surface brightness galaxies, and the relatively low quality of photometry for this class of galaxies makes the incompleteness significant; the completeness fraction of Im galaxies as read from Table 1 is only 54%, which is compared with $\approx 83\%$ for other classes of galaxies. Along with a small Im fraction, our sample for an appropriate redshift range is too small to derive a reliable MDLF for Im galaxies.

3. Morphology-Dependent Luminosity Functions

We show in Figure 1 the differential number counts of galaxies. The slope of the counts is slightly steeper than that of the Euclidean value, and is in agreement with previous studies (Yasuda et al. 2001). The counts of spectroscopic galaxies (indicated by the dashed curve) follow those of the photometric sample within one sigma of Poisson statistics, so that the completeness correction for the sample of the present paper does not depend on brightness.

We use the recession velocity with respect to the Galactic Standard of Rest according to RC3. We select galaxies in the redshift range $3000 \text{ km s}^{-1} < cz < 36000 \text{ km s}^{-1}$. The lower cutoff is imposed to avoid large effects from peculiar velocity flow, and the upper cutoff is practically the limit of our sample. We further impose a cut on apparent magnitude as $r^* \geq 13.2$ mag, since very bright galaxies are often dropped from spectroscopic targets. These selections exclude 71 galaxies from our sample, leaving 1482 galaxies used to estimate the MDLF. The redshift distributions of our galaxy sample are shown in Figure 2, where the curves show expectations for a homogeneous universe with the MDLF derived in this paper.

We compute MDLFs for the samples with three methods: maximum-likelihood (ML) (Sandage, Tammann & Yahil 1979), step-wise maximum-likelihood (SWML) (Efstathiou, Ellis & Peterson 1988) and the V_{max} method. We take the step of luminosity to be 0.25 mag for SWML. We adopt $\Omega = 0.3$ and $\lambda = 0.7$ for cosmology, although the maximum redshift of our sample is $z = 0.12$ and the results hardly depend on the cosmological parameters. The K correction is taken from Fukugita, Shimasaku & Ichikawa (1995) with an interpolation with respect to $g^* - r^*$ colour for each galaxy.

The results from the first two methods, ML and SWML, show a good agreement, but those from the V_{max} method differ from the former two in the faint end. This is a well-known effect generally ascribed to inhomogeneous galaxy distributions in the redshift space, as are visible in Figure 2. In Figure 3 we present the MDLF from ML and SWML in the r^* passband, together with the absolute magnitude distribution of galaxies used in the analysis. The ML estimate assumes the Schechter function

$$\phi(L)dL = \phi^* \left(\frac{L}{L_*} \right)^\alpha \exp \left[- \left(\frac{L}{L_*} \right) \right] \frac{dL}{L_*}, \quad (1)$$

and the derived parameters are given in Table 2, where we take the Hubble constant $h = H_0/100 \text{ km s}^{-1}\text{Mpc}^{-1}$. Only a crude estimate (with ML) is presented for the luminosity function for Im galaxies, since our sample is too small. We also present the results for the total sample, which includes not only galaxies with $T = 0 - 6$, but also those could not be classified ($T = -1$). This is a bright-galaxy version of the analysis given by Blanton et al.

(2001).

In this table we also give the luminosity densities obtained by integrating (1) over $L = 0$ to ∞ . The contours of one and two standard deviation errors calculated from the likelihood functions are shown in $\alpha - M^*$ plane in Figure 4. We have also carried out a jack-knife error estimate, by dividing the sample into ten RA bins (width of ~ 1.2 hr), in order to study the effect of the sample variance. The best-fit values for the subsamples all fall within the one-sigma ellipse given above, and the variance estimated from the jack-knife method is smaller than the error we quoted. So we adopt one-sigma of the fit for our final error estimate.

We then assign an additional 0.05 mag error from the calibration of photometry (added in quadratures). For more discussion about errors and selection effects, see Blanton et al. (2001). The errors expected from a number of items seen in their analysis are significantly smaller than the statistical error we are concerned with here.

We determine the normalization ϕ^* of the MDLF following the method of Efstathiou et al. (1988) for each sample of morphologically-classified galaxies. We adopt the region of M_{r^*} where the sample contains sufficient number of galaxies, dropping too bright ($M_{r^*} < M_{r^*}^* - 2$) and faint ($M_{r^*} > M_{r^*}^* + 1$) galaxies and those with high redshifts to avoid strong shot noise effects. We choose the redshift range to be $0.01 \leq z \leq 0.075$, for which the selection function for the total sample is $\gtrsim 0.14$. The numbers of galaxies used to determine ϕ^* are given in Table 1 above. In Table 2 we give jack-knife errors for ϕ^* . The normalization significantly varies depending on the cutoff of the redshift range, reflecting the presence of large-scale structure, such as a clump seen between $z = 0.07$ and 0.08 in Figure 2. The variation of the normalization by varying the upper cutoff between 0.07 and 0.08 is comparable to the jack-knife error we quoted. The normalizations (and errors) are then corrected for the sample incompleteness derived in Table 2 by comparing the spectroscopic sample with good-quality photometry and redshift determinations [(d) in Table 1] to the photometric sample [(a) in Table 1]. A small difference of areas covered by photometric and spectroscopic surveys is also taken into account. Furthermore, an extra correction factor of $(1875+88)/1875=1.05$ is multiplied to correct for the incompleteness of the photometric catalogue as discussed in section 2.

We can see following features in our luminosity functions:

(i) The characteristic luminosity and the faint end slope of the total sample are consistent with the parameters derived by Blanton et al. (2001) within 1–1.3 sigma. The normalization, however, is significantly lower, corresponding to by 30% in the luminosity density, than that of Blanton et al. This is ascribed to the local deficit of galaxies in the northern equatorial stripe seen for $r^* < 16$ mag, and is ascribed to large-scale structure, as discussed in Yasuda

et al. (2001). We confirmed that the normalization rapidly approaches that of Blanton et al. when we take the limiting magnitude fainter; with $r^* < 16.5$ mag, the luminosity density agrees with that of Blanton et al. within 10%.

(ii) The characteristic luminosity of early-type galaxies is more luminous than that of later-type galaxies by about 0.45 mag. This is consistent with the ‘universal characteristic luminosity’ known for the B band (Tammann, Yahil & Sandage 1979), because we expect that $B - r^*$ colour differs by 0.4 mag between E and Sb (Fukugita et al. 1995). This implies that the universal characteristic luminosity in the B band is an accidental effect.

(iii) The shape of the luminosity function of early-type galaxies is not much different from that of late-type galaxies, although some trend is seen that the number of early-type galaxies slightly declines ($\alpha \lesssim -1$) towards the faint end. This conclusion agrees with Marzke et al. (1994) for the B band, and Kochanek et al. (2001) for the K band, but does not agree with Loveday et al. (1992), which show an appreciable decline towards the faint end (see Zucca, Pozzetti & Zamorani 1994, which ascribe Loveday et al.’s result to a sample incompleteness). In particular, we do not see a sharp decline of the luminosity function, as inferred in Binggeli et al. (1988) and Bernardi et al. (2002a). The latter authors fit the luminosity function of early-type galaxies selected with photometric and spectroscopic parameters (Bernardi et al. 2002b)⁹ to a Gaussian function with a peak at $M_{r^*} = -20.38$ mag ($h = 1$): their data go beyond the peak only slightly, and the turn-over is not conclusive. Our luminosity function, which goes down to -18.75 mag, does not show any turnover to this magnitude.

(iv) The luminosity function of late-type spirals (Sbc-Sd) does not exhibit an increase ($\alpha \gtrsim -1$) towards the faint end. Our late-type spiral galaxy sample shows an even faster decline compared to that of early-type spiral galaxies. We found that the luminosity function derived from V_{\max} shows a somewhat faster increase ($\alpha = -1.16$) compared with those for other types, but this trend is not visible with the MDLF from the ML or SWML methods. We ascribe this larger α from the V_{\max} method to a local effect of the galaxy distribution, as we mention below. In any case the steepening of the faint end slope does not occur up to the Im type. This might appear to contrast with the conventional belief that late-type galaxies have a steep slope. This is due to our exclusion of very late galaxies ($T > 5$), and is consistent with Marzke et al. (1994), who found that only the Im luminosity function shows a steep faint end slope.

⁹These authors adopted selection criteria based on the concentration index ($C < 0.4$; see below), the PCA spectral classification index for early-type galaxies, and the de Vaucouleurs- versus exponential-likelihood parameters which are produced from the photometric pipeline. Note that the last parameter correlates very weakly with visual morphology; see Shimasaku et al. 2001.

(vi) The Im type luminosity function shows a steep faint end slope, $\alpha \sim -1.9$, consistent with Marzke et al.

It may be worth commenting that the absolute magnitude distributions of early- and late-type spiral galaxies shown in Figure 3 appear to indicate steeper faint end slope for the latter. This is in fact what we have obtained when we use the V_{\max} method. This reflects the effect seen in Figure 2 that the morphological composition appears to change as a redshift [i.e., the frequency of late-type spirals is high in nearby ($z < 0.05$) sample]. This effect disappears when we use the likelihood method to calculate the luminosity function *under the assumption that it is universal*.

For practical uses of the MDLF presented here, the normalization should be multiplied by a factor of 1.29 to correct for the local deficit of galaxies in the northern equatorial stripe in brighter magnitudes.

4. Morphological classification with the concentration index

The luminosity function of early-type galaxies we derived does not show a conspicuous decline towards the faint end. One may suspect that that our E and S0 sample may contain increasingly more dwarf ellipticals and spheroidals, which are not separated from their giant counterparts in visual classifications, towards the faint end, and therefore the luminosity function of giant elliptical galaxies might actually decline.

This point may be studied by using a concentration index, since early-type dwarfs usually have galaxy cores significantly softer than those of giant elliptical galaxies (e.g., Kormendy 1986). We define the (inverse) concentration index by the ratio of the two Petrosian radii $C = r_{50}/r_{90}$ measured in the r^* band, where r_{50} and r_{90} are radii which correspond to the apertures that include 50% and 90% of the Petrosian flux. In Figure 5 we plot C as a function of absolute magnitudes for E and S0 galaxies. The plot shows that there is no evident trend that fainter early-type galaxies have softer cores; most of the data points fall below $C < 0.34$, which is a typical value that divides early and late types, down to -19 mag.

Shimasaku et al. (2001) report that this C parameter shows the strongest correlation with visually-classified morphology among simple photometrically-defined parameters (see also, Doi, Fukugita & Okamura 1993; Abraham et al. 1994; Blanton et al. 2001; Strateva et al. 2001; Bernardi et al. 2002b). We thus separate morphologies into early and late types according as $C < 0.35$ or $C > 0.35$, which corresponds to the division at S0/a. The early-type galaxy sample (706 galaxies) thus defined shows a 82% completeness and is contaminated by late-type galaxies by 18% when we take the visually-classified sample as the reference. The

late-type sample (713 galaxies) also shows a 82% completeness and a 18 % contamination from the opposite sample. This choice of C minimizes the contamination of the opposite morphologies either way. The analysis is similar to what was already presented by Blanton et al. (2001), with the difference that they have used $C = 0.43$ (which corresponds to Sb for bright galaxies) to divide the early- and late-type galaxy samples.

Figure 6 shows the MDLF separated according to this C index. The parameters of the Schechter function from the ML analysis are given in Table 3 above. The use of a different division at $C = 0.34$, which is about the division at S0 galaxies, changes the MDLF only slightly. The feature of the luminosity functions is similar to what are derived from the visually-classified sample. The MDLF for early-type galaxies shows a characteristic luminosity brighter than that for late-types, and has a slightly declining faint-end shape while late-type galaxies show a flat faint end. No sharp decline of the luminosity function is visible at least two mag fainter than M^* , or at least 2 mag fainter than the peak inferred by Bernardi et al. (2002a).

Our result means that it is unlikely that the visually-classified sample is dominated by dwarf ellipticals that have soft cores in faint magnitudes. The luminosity function of late-type galaxies also shares the features of the visually-classified late-type galaxy sample. This analysis shows that the MDLFs using the concentration index are similar to those with visually-classified samples, although a somewhat smaller difference of characteristic luminosities of the two types represents the $\sim 20\%$ contamination from the opposite types.

5. Conclusions

Our sample is small and we may not be able to extract quantitatively robust parameters, yet we obtain a number of useful conclusions. The most important feature with our analysis is that we have used a homogeneous photometric catalogue with sharply defined selection criteria and a homogeneously morphologically-classified sample based on Hubble morphology of galaxies, rather than a sample classified by indicators using spectroscopic features or colours, which are sensitive to small star formation activities in the present or the near past.

The first conclusion we have obtained is that the shape of the MDLF does not depend too strongly on the Hubble types. The characteristic luminosity of elliptical and S0 galaxies is brighter than that of spiral galaxies in the r^* band. The amount of the difference in brightness is consistent with universal characteristic luminosity in the B band, which was found by Tammann et al. (1979). The MDLF of early-type galaxies somewhat declines in the faint end, but does not exhibit a sharp decline, and this is not due to an increasing mixture

of dwarf galaxies at least in the magnitude range we are concerned with. The conclusion is unchanged if we use the concentration index as a classifier of early-type galaxies. This indicates that there are many intrinsically faint elliptical galaxies, whose luminosities are fainter than those of bulges in spiral galaxies. The existence of numerous early-type galaxies with a hard core at small luminosities indicates that morphology is unlikely to be a sequence of the bulge luminosity as advocated by Dressler & Sandage (1983), and by Meisels and Ostriker (1984). Our conclusion also justifies the calculation of the strong gravitational lensing frequency of quasars using the standard Schechter function without introducing a cutoff in the luminosity function, which would affect the frequency of sub-arcsecond lensing.

Funding for the creation and distribution of the SDSS Archive has been provided by the Alfred P. Sloan Foundation, the Participating Institutions, the National Aeronautics and Space Administration, the National Science Foundation, the U.S. Department of Energy, the Japanese Monbukagakusho, and the Max Planck Society. The SDSS Web site is <http://www.sdss.org/>. The SDSS is managed by the Astrophysical Research Consortium (ARC) for the Participating Institutions. The Participating Institutions are The University of Chicago, Fermilab, the Institute for Advanced Study, the Japan Participation Group, The Johns Hopkins University, Los Alamos National Laboratory, the Max-Planck-Institute for Astronomy (MPIA), the Max-Planck-Institute for Astrophysics (MPA), New Mexico State University, University of Pittsburgh, Princeton University, the United States Naval Observatory, and the University of Washington. We would like to thank Sadanori Okamura for useful comments. MF is supported in part by the Grant in Aid of the Japanese Ministry of Education.

REFERENCES

- Abraham, R. G., Valdes, F., Yee, H. K. C., & van den Bergh, S. 1994, *ApJ*, 432, 75
- Bernardi et al. 2002a, to be published in *AJ*
- Bernardi et al. 2002b, to be published in *AJ*
- Binggeli, B., Sandage, A. & Tammann, G. A. 1988, *ARAA*, 26, 509
- Blanton, M. et al. 2001, *AJ*, 121, 2358
- Bromley, B. C. 1998, *ApJ*, 505, 25
- Doi, M., Fukugita, M., & Okamura, S. 1993, *MNRAS*, 264, 832
- Dressler, A. & Sandage, A. 1983, *ApJ*, 265, 664
- Efstathiou, G., Ellis, R. S. & Peterson, B. A. 1988, *MNRAS*, 232, 431
- Folkes, S. et al. 1999, *MNRAS*, 308, 459
- Fukugita, M., Ichikawa, T., Gunn, J. E., Doi, M., Shimasaku, K., & Schneider, D. P. 1996, *AJ*, 111, 1748
- Fukugita, M., Shimasaku, K., & Ichikawa, T. 1995, *PASP*, 107, 945
- Fukugita, M. & Turner, E. L. 1991, *MNRAS*, 253, 99
- Gunn, J. E. et al. 1998, *AJ*, 116, 3040
- Hogg, D. W., Finkbeiner, D. P., Schlegel, D. J., and Gunn, J. E. 2001, *AJ*, 122, 2129
- Kochanek, C. S. et al. 2001, *ApJ*, 560, 566
- Kormendy, J. 1986, in *Nearly Normal Galaxies*, ed. S. M. Faber (New York: Springer-Verlag), p. 163
- Loveday, J., Peterson, B. A., Efstathiou, G & Maddox, S. J. 1992, *ApJ*, 390, 338
- Marzke, R. O., Geller, M. J., Huchra, J. P. & Corwin, Jr. H. G. 1994, *AJ*, 108, 437
- Marzke, R. O., da Costa, L. N., Pellegrini, P. S., Willmer, C. N. A., & Geller, M. J. 1998, *ApJ*, 503, 617
- Meisels, A. & Ostriker, J. P. 1984, *AJ*, 89, 1451
- Pier, J. R. et al. 2002, submitted to *AJ*
- Sandage, A. 1961, *The Hubble Atlas of Galaxies*. Carnegie Institution of Washington, Washington DC
- Sandage, A., Tammann, G. A. & Yahil, A. 1979, *ApJ*, 232, 352
- Schlegel, D. J., Finkbeiner, D. P. & Davis, M. 1998, *ApJ*, 500, 525

- Shimasaku, K. et al. 2001, AJ, 122, 1238
- Smith, J. A. et al. 2002, ApJ, 123, 2121
- Stoughton, C. et al. 2002, AJ, 123, 485
- Strateva, I. et al. 2001, AJ, 122, 1861
- Strauss, M. A. et al. 2002, AJ, 124, 1810
- Tammann, G. A., Yahil, A. & Sandage, A. 1979, ApJ, 234, 775
- de Vaucouleurs, G., de Vaucouleurs, A., Corwin, H., Buta, R., Paturel, G., & Fouqué, P.
1991, Third Reference Catalogue of Bright Galaxies (Springer, New York) (RC3)
- Yasuda, N. et al. 2001, AJ, 122, 1104
- York, D. G. et al. 2000, AJ, 120, 1579
- Zucca, E., Pozzetti, L. and Zamorani, G. 1994, MNRAS, 269, 953

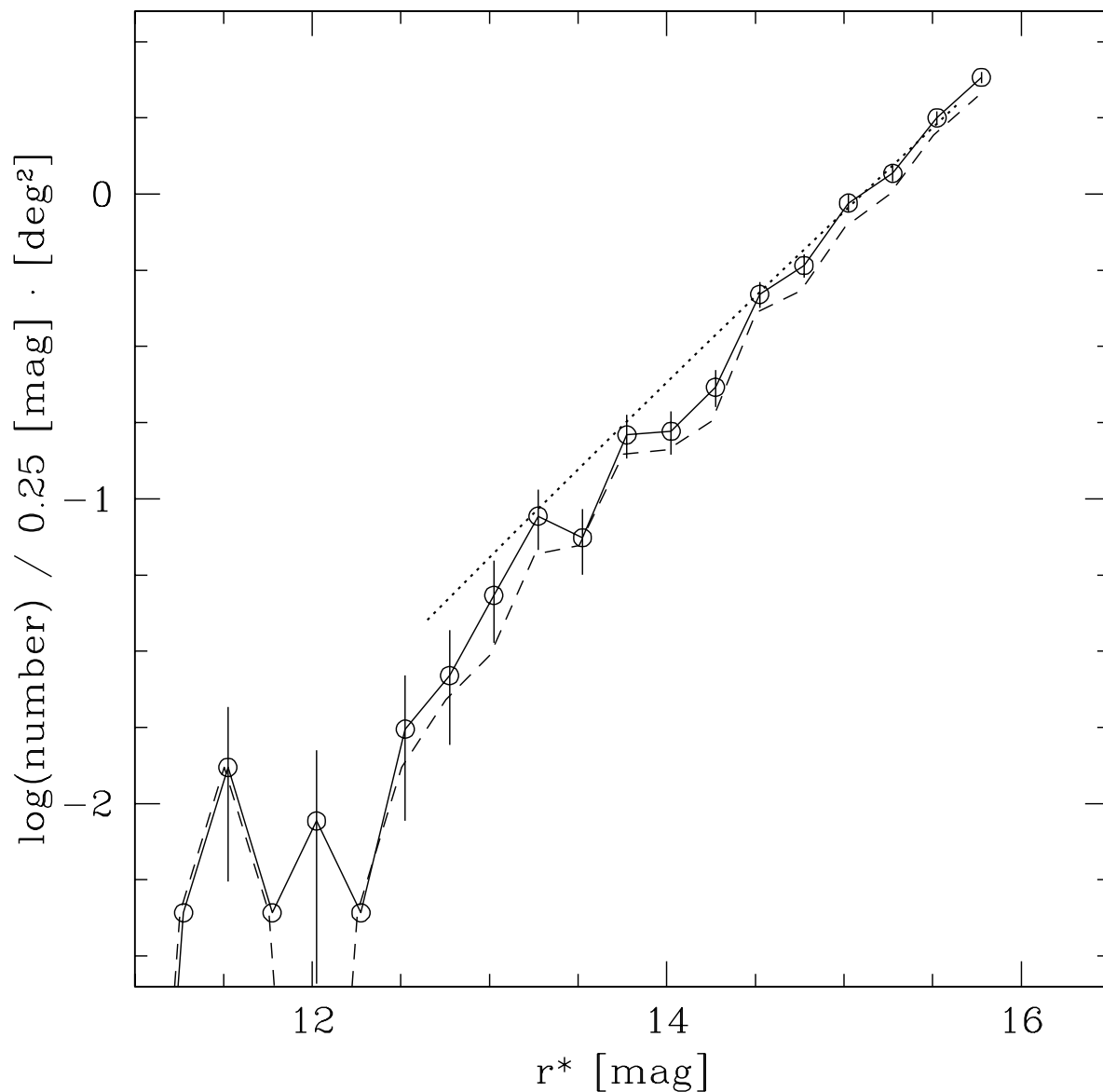


Fig. 1.— Differential galaxy number counts in the r^* band as a function of magnitude. The dashed curve is the spectroscopic sample, which is compared with the photometric sample represented by the solid curve. The dotted curve is the prediction from the luminosity function obtained in this paper, showing a deficiency of galaxies in bright magnitudes for the northern equatorial stripe.

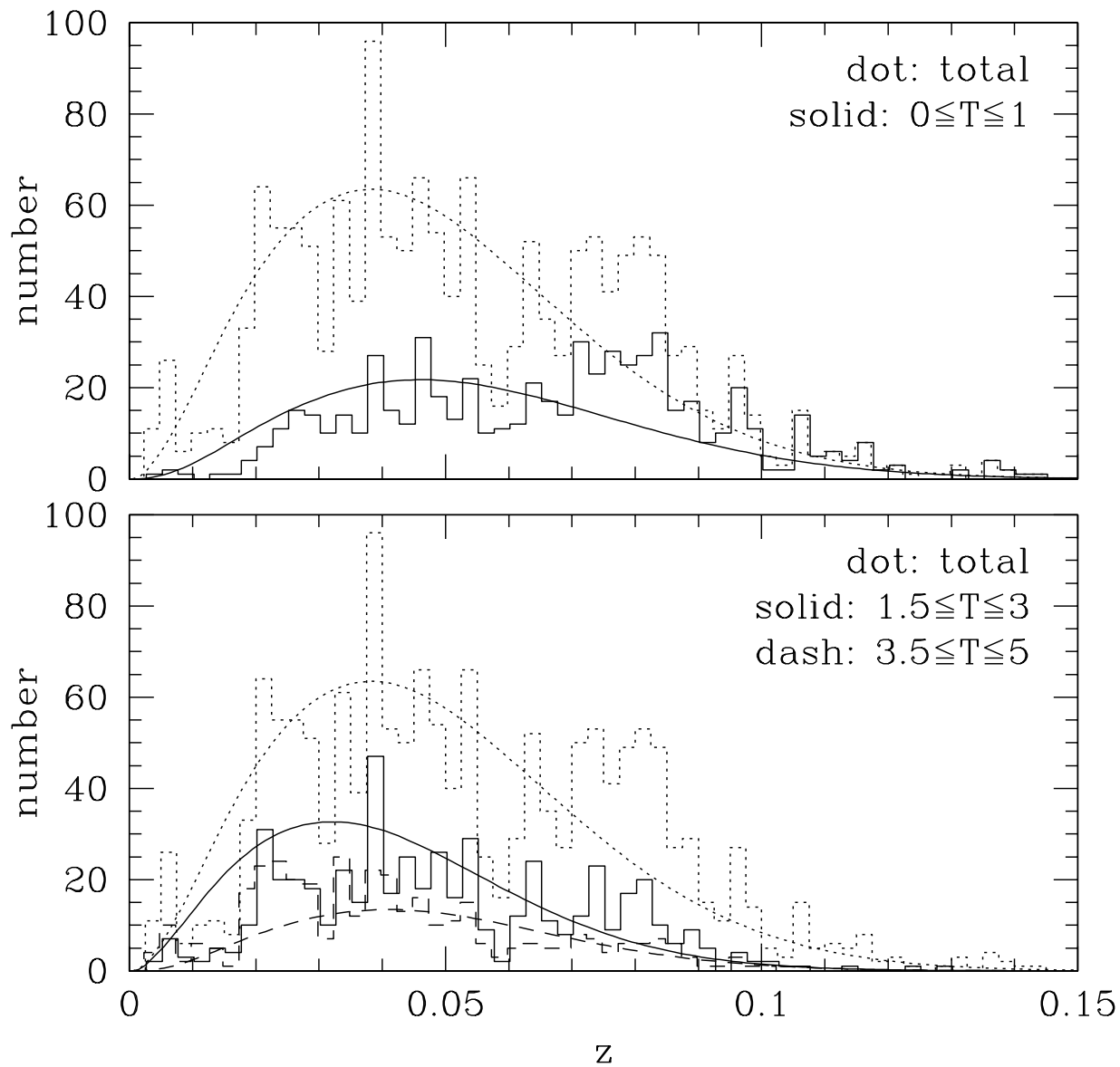


Fig. 2.— The redshift distribution of galaxies, compared with the predictions for the homogeneous universe calculated with the MDLF we obtain in this paper. The upper panel is for early-type (E and S0) galaxies, and the lower panel for later type (S0/a-Sb; Sbc-Sd) galaxies. The dashed curves show the total sample.

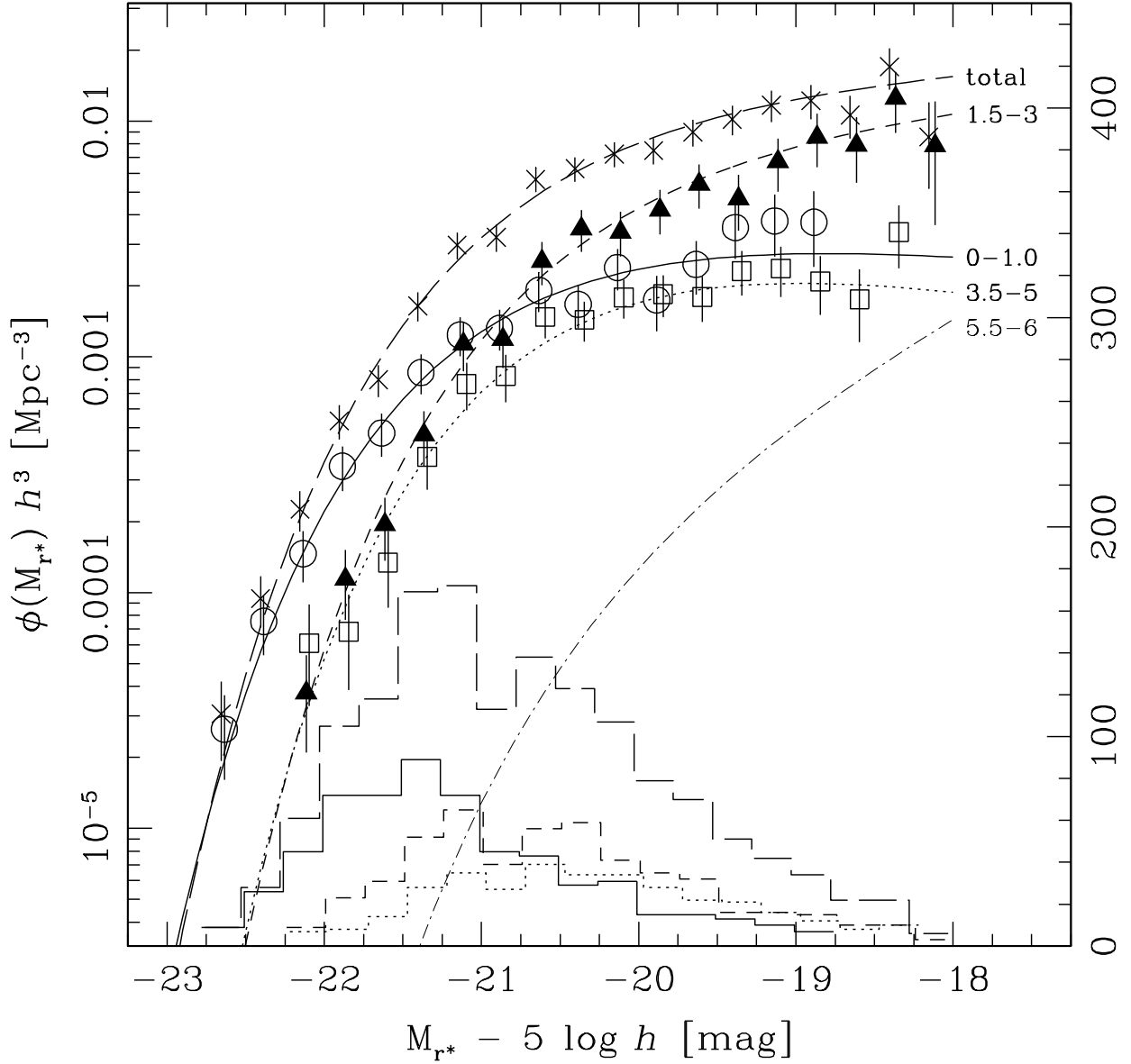


Fig. 3.— MDLF in the r^* band for three types, E-S0, S0a-Sb, and Sbc-Sd from visual classifications. The SWML results are represented by data points (open circle for E-S0; solid triangle for early spiral galaxies; open square for late-type spiral galaxies), and the ML fits are shown by solid, short dashed and dotted curves, respectively. The ML estimate for Im galaxies is represented by dash-dotted curve. The luminosity function for the total sample is also plotted for comparison, represented by crosses and a long-dashed curve. The histograms are the actual numbers of galaxies for the three types and the total sample used in this analysis.

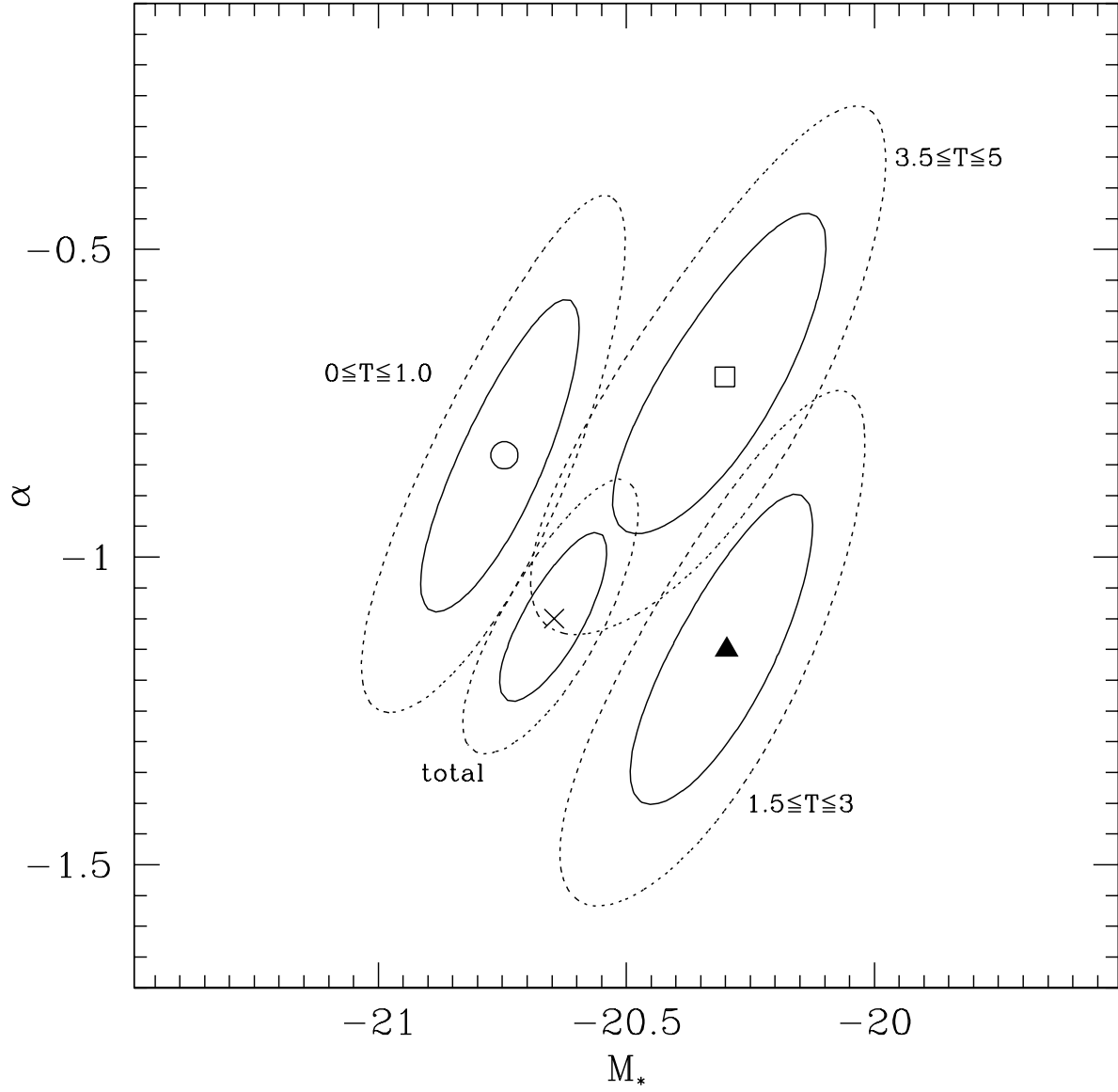


Fig. 4.— Error contours (solid curve for 1 sigma, dotted curve for 2 sigma) of the parameters of the Schechter functions for the ML fits given in Figure 3. The unit of the abscissa assumes $h = 1$.

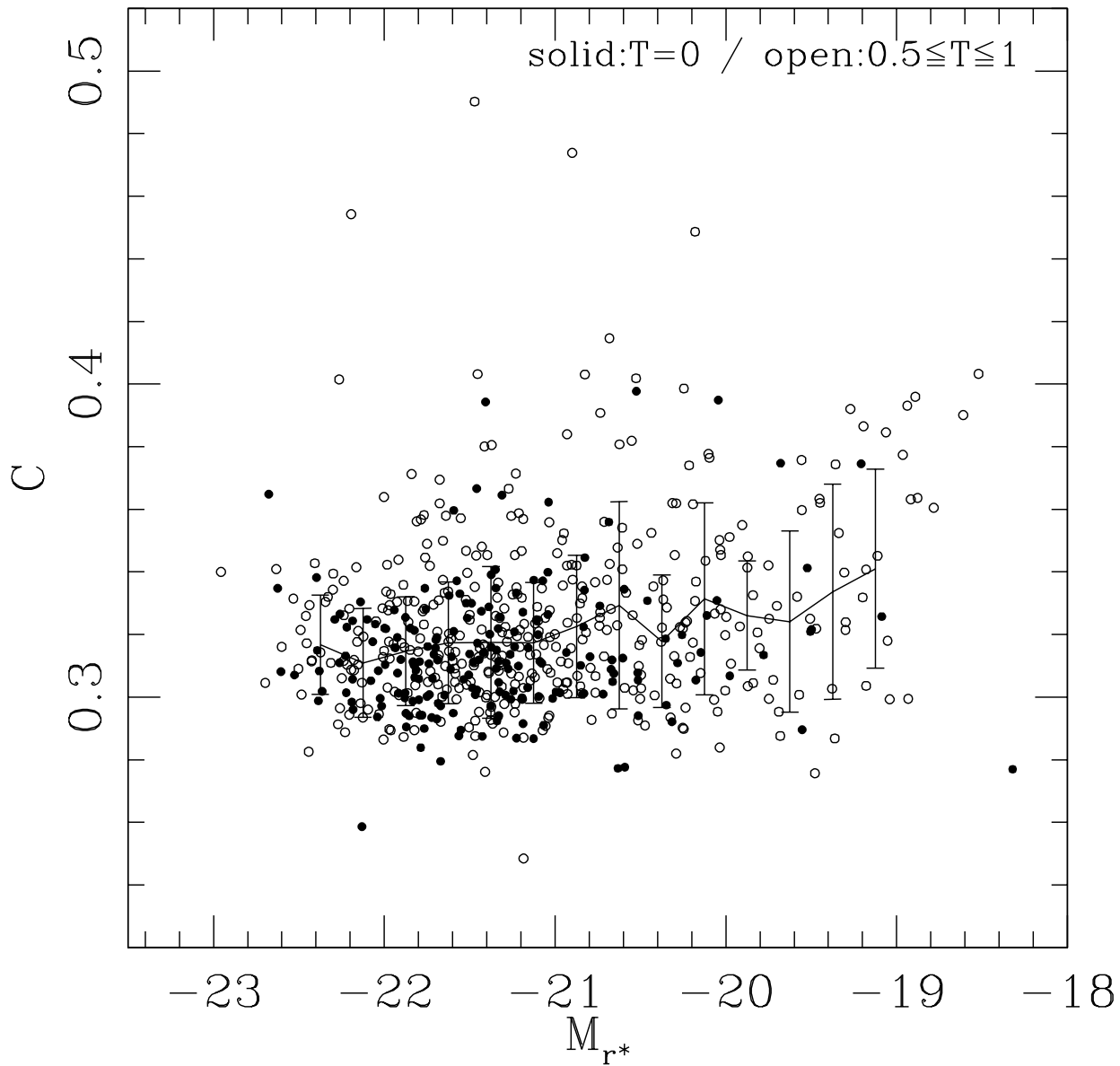


Fig. 5.— Concentration indices of early-type galaxies plotted as a function of absolute magnitudes. Solid points are galaxies classified as E and open points are other early-type galaxies (E/S0 or S0). The average of C as a function of luminosity is also given. The unit of the abscissa assumes $h = 1$.

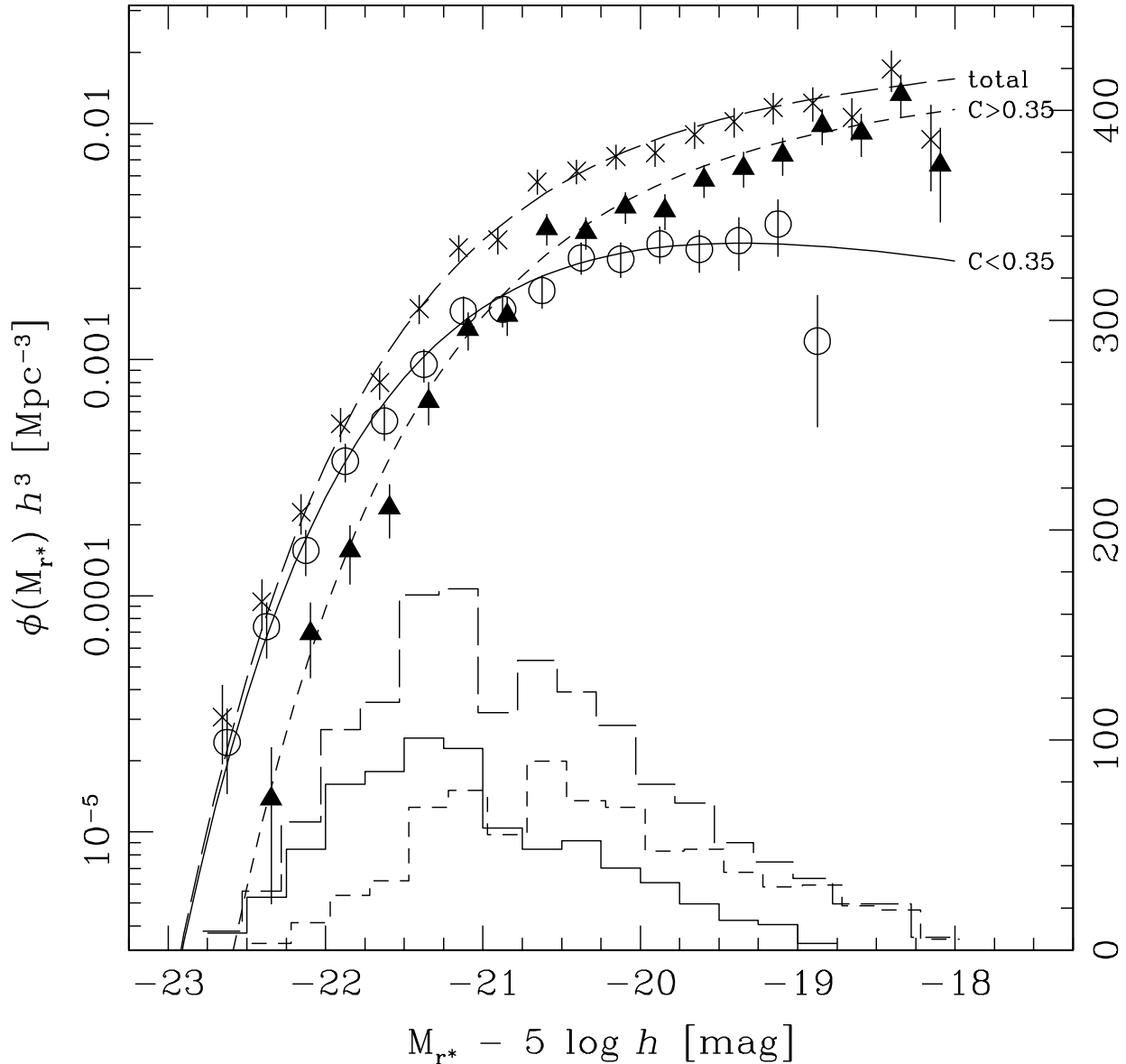


Fig. 6.— MDLF for early and late-type galaxies classified using the concentration index. The SWML results are represented by data points (open circle for early-type with $C < 0.35$; solid triangle for late type $C > 0.35$), and the ML fits are shown by solid and short dashed curves, respectively. The luminosity function for the total sample is plotted for comparison, represented by crosses and a long-dashed curve. The histograms are the numbers of galaxies used in this analysis.

Table 1: Morphologically classified sample

| | $0 \leq T \leq 1$ (E & S0) | $1 < T \leq 3$ (S0/a-Sb) | $3 < T \leq 5$ (Sbc-Sd) | $5 < T \leq 6$ (Im) | $T = -1$ (unclass.) | total |
|---------------------------------------|-------------------------------|-----------------------------|----------------------------|------------------------|------------------------|-------|
| (a) photometric sample | 740 | 630 | 444 | 35 | 26 | 1875 |
| (b) spectroscopic sample | 630 | 545 | 381 | 23 | 21 | 1600 |
| (c) sample with good photometry | 617 | 539 | 373 | 21 | 12 | 1562 |
| (d) sample with z ($\geq 85\%$ CL) | 616 | 538 | 369 | 19 | 11 | 1553 |
| (e) sample used in MDLF | 597 | 518 | 350 | (10) | (7) | 1482 |
| (f) sample used to give ϕ^* | 314 | 368 | 253 | (5) | | 894 |

Table 2: Luminosity function parameters

| morphology | $M^*(r^*) - 5 \log h$ | α | ϕ^* ($0.01h^3\text{Mpc}^{-3}$) | $\mathcal{L}(r^*)$ ($10^8hL_\odot \text{Mpc}^{-3}$) |
|---------------------|-----------------------|------------------|--|--|
| total | -20.65 ± 0.12 | -1.10 ± 0.14 | 1.43 ± 0.21 | 2.00 |
| $0 \leq T \leq 1.0$ | -20.75 ± 0.17 | -0.83 ± 0.26 | 0.47 ± 0.09 | 0.62 |
| $1.5 \leq T \leq 3$ | -20.30 ± 0.19 | -1.15 ± 0.26 | 0.95 ± 0.15 | 1.00 |
| $3.5 \leq T \leq 5$ | -20.30 ± 0.20 | -0.71 ± 0.26 | 0.43 ± 0.05 | 0.37 |
| $5.5 \leq T \leq 6$ | ~ -20.0 | -1.9 | ~ 0.04 | |
| $C < 0.35$ | -20.62 ± 0.14 | -0.68 ± 0.23 | 0.67 ± 0.12 | 0.76 |
| $C > 0.35$ | -20.35 ± 0.19 | -1.12 ± 0.18 | 1.09 ± 0.14 | 1.17 |